methods

The biotin-capture lipid affinity assay: a rapid method for determining lipid binding parameters for apolipoproteins

W. Sean Davidson,[1] Amy B. Ghering, Lauren Beish, Matthew R. Tubb, David Y. Hui, and Kevin Pearson

Department of Pathology and Laboratory Medicine, University of Cincinnati, Cincinnati, OH 45237-0507

Abstract **The lipid affinity of plasma apolipoproteins is an important modulator of lipoprotein metabolism. Mutagenesis techniques have been widely used to modulate apolipoprotein lipid affinity for studying biological function, but the approach requires rapid and reliable lipid affinity assays to compare the mutants. Here, we describe a novel method that measures apolipoprotein binding to a standardized preparation of small unilamellar vesicles (SUVs) containing trace biotinylated and fluorescent phospholipids. After a 30 min incubation at various apolipoprotein concentrations, vesicle-bound protein is rapidly separated from free protein on columns of immobilized streptavidin in a 96-well microplate format. Vesicle-bound protein and lipid are eluted and measured in a fluorescence microplate reader for calculation of a dissociation constant and the maximum number of potential binding sites on the SUVs. Using human apolipoprotein A-I (apoA-I), apoA-IV, and mutants of each, we show that the assay generates binding constants that are comparable to other methods and is reproducible across time and apolipoprotein preparations. The assay is easy to perform and can measure triplicate binding parameters for up to 10 separate apolipoproteins in 3.5 h, consuming only 120 μg of apolipoprotein in total. The benefits and potential drawbacks of the assay are discussed.**—Davidson, W. S., A. B. Ghering, L. Beish, M. R. Tubb, D. Y. Hui, and K. Pearson. **The biotin-capture lipid affinity assay: a rapid method for determining lipid binding parameters for apolipoproteins. *J. Lipid Res.* 2006.** 47: **440–449.**

Supplementary key words lipid binding assay • fluorescence • small unilamellar vesicle • biotin/streptavidin

Plasma apolipoproteins are critical players in lipid metabolism. They emulsify insoluble lipid molecules into small packages (i.e., lipoproteins) for transport in aqueous plasma. In addition, they impart functionality and directionality by acting as modulators for a host of lipases, transfer proteins, cell surface binding proteins, and proteoglycans. The family of exchangeable apolipoproteins that includes apolipoprotein A-I (apoA-I), apoA-II, and apoA-IV can exist in a stable lipid-free state after secretion or when moving between lipoproteins. Recent evidence suggests that these lipid-dissociated forms may be capable of distinct functions. For example, lipid-free apoA-I can interact with the cell surface ABCA1 to promote the cellular efflux of lipids to form nascent HDL particles (for a recent review, see 1). By contrast, HDL-bound apoA-I, although capable of promoting lipid efflux via several additional mechanisms (2, 3), fails to interact with ABCA1 (4). A related protein, apoA-IV, may exist in the lipid-dissociated state to a greater extent [up to 50% of its mass (5)], but the function(s) of this form is not yet clear.

Given the importance of apolipoproteins and their transitions in lipid metabolism, we have begun to study the structural and biological consequences of lipid binding affinity using mutagenesis strategies (6, 7). Our goal has been to produce apolipoprotein mutants with variable lipid affinities and then measure the impact on indices of apolipoprotein function both in vitro and in vivo. The generation of a large number of apolipoprotein mutants for these studies has created a need for a robust method to characterize the lipid affinities of the variants in a rapid but statistically rigorous manner.

Numerous methods have been developed to quantitate apolipoprotein lipid affinity. The more sophisticated strategies include the use of calorimetry (8–12), surface chemistry (13, 14), oil-drop tensiometry (15), capillary electrophoresis (16), or resonance energy transfer (17, 18). These methodologies can characterize the lipid binding reaction in great detail. For instance, isothermal titration calorimetry can derive affinity constants and changes in enthalpy, entropy, and heat capacity for apolipoprotein binding to lipid

Manuscript received 19 September 2005 and in revised form 1 November 2005.

Published, JLR Papers in Press, November 2, 2005.
DOI 10.1194/jlr.D500034-JLR200

Abbreviations: apoA-I, apolipoprotein A-I; BCLA, biotin-capture lipid affinity; BT-PE, (biotinyl)-1,2-dipalmitoyl phosphatidylethanolamine; Dansyl-PE, (5-dimethylamino-1-naphthanesulfonyl)-1,2 dioleoylphosphatidylethanolamine; DMPC, dimyristoylphosphatidylcholine; K_d, equilibrium dissociation constant; n, maximal binding of an apolipoprotein to a given lipid surface; PL, phospholipid; POPC, 1-palmitoyl,2-oleoyl phosphatidylcholine; Rhod-PE, (*N*-lissamine rhodamine B sulfonyl)-1,2 dioleoyl phosphatidylethanolamine; SUV, small unilamellar vesicle.

[1] To whom correspondence should be addressed.
e-mail: sean.davidson@uc.edu

emulsions or synthetic vesicles. Although tremendously useful for analyzing limited numbers of proteins, most of these methods require the analysis of multiple apolipoprotein concentrations that must be run in a serial manner. Thus, the measurement of replicate data sets for a given apolipoprotein can take hours to days depending on the method, making them less attractive for comparing larger sample sets. In addition, these methods require sophisticated and expensive instrumentation. There are also less sophisticated methods, such as vesicle lysis (19) and turbidometric, colorimetric (20), and physical separation assays (21). Many of these are straightforward, rapid, and require relatively common instrumentation. However, most do not allow the determination of useful equilibrium binding coefficients. For example, one of the most widely used methods for comparing apolipoprotein lipid ''affinity'' is the dimyristoylphosphatidylcholine (DMPC) liposome disruption assay (22). Although this assay has proven useful for qualitative comparisons between proteins, the complex nature of the lipid solubilization reaction (23) and the fact that rates are usually measured at a single ratio of protein to lipid precludes the determination of generally applicable binding parameters, such as an equilibrium dissociation constant (K_d) or the maximal binding of an apolipoprotein to a given lipid surface (n) (see Discussion). One method capable of deriving these parameters was described by Yokoyama et al. (21). They used small gel filtration columns to physically separate vesicles with bound apolipoprotein from unbound protein, followed by quantification of phospholipid (PL; by radioactivity) and protein (by fluorescence assay). However, because their method relies on relatively slow gel filtration separations for each sample in a multiple concentration experiment, the analysis is time-consuming and tedious for even a few samples.

To circumvent some of these issues, we set out to develop a simple lipid affinity assay that *a*) allows for the reproducible calculation of K_d and n for apolipoproteins binding to a uniform lipid surface; *b*) allows the analysis, in triplicate, of at least 5–10 apolipoproteins in a single experiment; and *c*) consumes minimal amounts of protein sample. The resulting method (illustrated in **Fig. 1**) measures apolipoprotein binding to a standardized set of small unilamellar vesicles (SUVs) containing trace amounts of biotinylated and fluorescent PLs. We characterize this biotin-capture lipid affinity (BCLA) assay below.

EXPERIMENTAL PROCEDURES

Materials and equipment

1-Palmitoyl,2-oleoyl phosphatidylcholine (POPC), (biotinyl)-1,2-dipalmitoyl phosphatidylethanolamine (BT-PE), (*N*-lissamine rhodamine B sulfonyl)-1,2 dioleoyl phosphatidylethanolamine (Rhod-PE), and (5-dimethylamino-1-naphthanesulfonyl)-1,2 dioleoylphosphatidylethanolamine (Dansyl-PE) were purchased

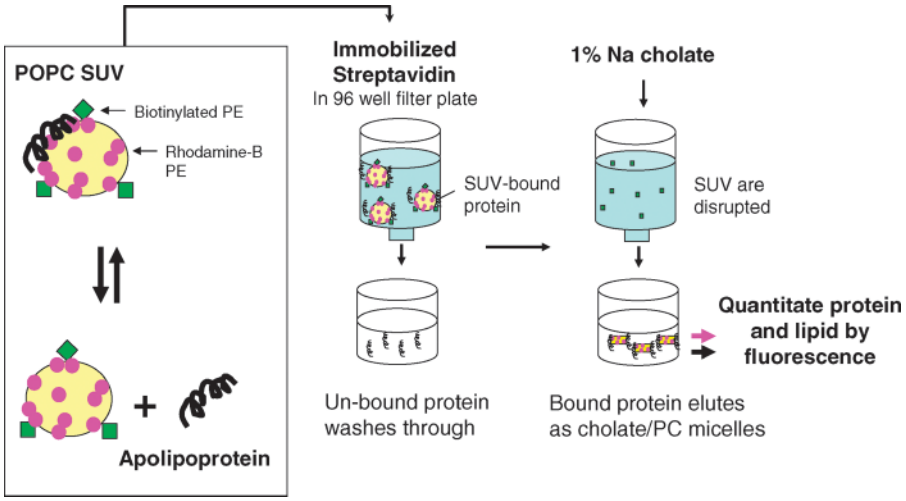

Fig. 1. General scheme of the lipid binding assay. Small unilamellar vesicles (SUVs) containing 99% (w/w) 1-palmitoyl,2-oleoyl phosphatidylcholine (POPC), 0.5% (biotinyl)-1,2-dipalmitoyl phosphatidylethanolamine (BT-PE; biotinylated PE) (green squares), and 0.5% (*N*-lissamine rhodamine B sulfonyl)-1,2 dioleoyl phosphatidylethanolamine (Rhod-PE; rhodamine-B PE) (pink circles) are prepared by sonication and mixed with increasing amounts of the apolipoprotein being assayed. After a 30 min incubation at 25°C, this solution contains a distribution of lipid-free and lipid-bound protein. The fraction of lipid-bound protein is measured by applying the sample to an immobilized streptavidin column in a 96-well format and incubating for 30 min. The vesicles are retained on the column via the biotin/streptavidin interaction along with any associated protein. Unbound protein passes though the column in a brief wash. The lipid-bound protein is then eluted by adding a solution of 1% sodium cholate, which solubilizes the nonbiotinylated phospholipid (PL) and protein into small micelles that pass onto a 96-well fluorescence mircoplate. The eluted protein is quantitated using the CBQCA fluorescence assay, and the total bound PL is measured from the residual rhodamine B fluorescence. Both measurements are performed simultaneously using a fluorescence plate reader. The data are then analyzed to determine an equilibrium dissociation constant (K_d) and a total number of binding sites (n) per vesicle (see Appendix).

from Avanti Polar Lipids (Birmingham, AL). The atomic phosphorus standard and sodium cholate were obtained from Sigma (St. Louis, MO). Immobilized streptavidin was obtained from Pierce (Rockford, IL; Ultralink 53114) or BioPlus (Dublin, OH; streptavidin Sepharose 506916). Ninety-six-well filter plates (1.2 μM, hydrophilic, low protein binding; MABVNOB10) were from Millipore (Billerica, MA), and black 96-well fluorescence assay plates were from Corning (Acton, MA). The 3-(4-carboxybenzoyl)quinoline-2-carboxaldehyde (CBQCA) fluorescence protein assay kit was obtained from Molecular Probes/Invitrogen (Carlsbad, CA). All other reagents were analytical grade.

To separate SUV-associated protein from unassociated protein, a 96-well filter plate and a vacuum manifold are used to rapidly load, wash, and elute microcolumns of immobilized streptavidin directly onto a standard 96-well fluorescence microplate for analysis. Our system was from Millipore; however, numerous systems are commercially available. A fluorescence microplate reader is required that is capable of exciting rhodamine B (excitation, 550 nm; emission, 590 nm) and the CBQCA product (excitation, 465 nm; emission, 550 nm). Finally, although not strictly required, a precision eight channel pipettor with a volume capacity of 50–300 μl dramatically increases the speed and precision of the column manipulations.

Methods

Generation and/or purification of apolipoproteins. Human apoA-I and apoA-II purification from normal human plasma was carried out as reported previously (24, 25). Recombinant apolipoproteins, including mutants of human apoA-I (6) and wild-type and mutated forms of human apoA-IV, were expressed in *Escherichia coli* and purified as described previously (7). All apolipoproteins in this study were denatured in 3 M guanidine HCl and refolded by dialysis against PBS (pH 7.8) before use.

Preparation of SUVs for binding studies. The standard vesicle preparation for most experiments described here contained the following composition: 99% POPC, 0.5% BT-PE, and 0.5% Rhod-PE (w/w). Variations on this composition for specific experiments are noted where appropriate in the figure legends. Vesicles were typically prepared in 60 mg batches in a borosilicate tube with lipids in chloroform stock. The chloroform was completely removed by evaporation under nitrogen for 16 h. Two milliliters of PBS was added, the tube was vortexed until the lipid was in suspension, and the sample was pulse-sonicated on ice using a Fisher Biosciences probe sonicator for 1 h with a 1 s on/1 s off duty cycle at ~75% of the probe's maximum setting. The vesicles were then centrifuged at maximum in a microcentrifuge for 20 min to pellet any unreacted lipid and titanium residue from the sonicator. The preparation was applied to a Superose 6 gel filtration column (Amersham Biosciences) equilibrated in PBS (26). Fractions corresponding to SUVs were then concentrated by ultrafiltration and quantitated by analysis of phosphorus, taking care to run blanks for the background phosphorus present in the PBS. The vesicles were stored capped under nitrogen at room temperature in the dark until used. We found that these preparations can be stored for up to 4 months with no loss of solubility or performance in the assay.

Lipid binding assay general protocol. The general scheme of the assay is illustrated in Fig. 1. The assay is performed by incubating seven concentrations of apolipoprotein with a fixed mass of SUV (43 μg of PL) in a volume of 100 μl of PBS. To statistically compare the binding parameters, each binding curve is performed in triplicate. A typical experimental setup with human plasma apoA-I is shown in **Table 1**. A range of apoA-I masses from 0 to 22.5 μg per 100 μl is used. To increase precision, the triplicates are prepared in one solution and then split when applied to the columns. The PBS and vesicles should be mixed first, followed by addition of the apolipoprotein. The additional 15 μl "fudge" volume was calculated in for pipetting errors. In addition, a vesicle control is also prepared that contains PBS/1% sodium cholate for comparison with the eluted samples (see below). These samples and standard can be prepared in glass test tubes or in microplate wells to facilitate transfer to the columns with a multipipettor. Once prepared, the samples are vortexed and incubated for 30 min at room temperature. Meanwhile, immobilized streptavidin columns are prepared on a 96-well filter plate by adding 50 μl of streptavidin resin in the appropriate number of wells (this results in ~ 25–30 μl of actual resin per well once the storage solution is removed). Using a vacuum manifold, the storage buffer is pulled through the resin and discarded. The resin is then washed with 250 μl of PBS, vortexed lightly, and then aspirated. Repeat the wash three times. After removing the last wash, 100 μl of each sample is added to the resin and incubated for 30 min. Note that the vesicle control sample is not added to the wells at this time. If available, a plate shaker set on a low speed should be used. Alternatively, the plate can be lightly vortexed every 10 min. After the incubation period, the resin is aspirated and the flow-through is discarded. Each well is rapidly washed two times with 100 μl of PBS, aspirated, and discarded. The streptavidin resin now contains bound vesicles and any vesicle-associated protein by virtue of the biotinylated lipid present in the SUV. The protein and PL are then eluted from the column by adding 100 μl of PBS with 1% sodium cholate (w/v). (Note: do not use other detergents such as SDS or Triton X-100 for the elution step. We found that SDS knocks the streptavidin off the column and Triton X-100 disrupts the surface tension, interfering with sample aspiration in the manifold.) The excess of detergent emulsifies the protein and the nonbiotinylated PLs into micelles that can pass though the column. The filter plate is gently vortexed, then aspirated onto a clean, black fluorescence-compatible microplate. This is followed by a 100 μl wash and then a final 50 μl wash with the same buffer. The final volume in each well of the microplate should be 250 μl. At this point, the vesicle control prepared as shown in Table 1 should be pipetted into empty wells on the plate (not passed through a column) and then brought to the same volume as the other samples with an additional 150 μl of PBS/1% sodium cholate. These wells will be used to determine the fluorescence intensity for the entire 43 μg

TABLE 1. A typical experimental setup for the analysis of human plasma apoA-I using the lipid binding assay

ApoA-I (μg per 100 μl sample)	Protein for Three Samples[a]	SUV for Three Samples[b]	PBS for Three Samples	Total for Three Samples[c]
	μl			
0 (0 μM)	0	7.9	307.1	315
1 (0.4 μM)	2.8	7.9	304.3	315
2.5 (0.9 μM)	7.0	7.9	300.1	315
5 (1.8 μM)	14.1	7.9	293.0	315
10 (3.6 μM)	28.1	7.9	279.0	315
15 (5.4 μM)	42.2	7.9	264.9	315
22.5 (8.0 μM)	63.3	7.9	243.8	315

apoA-I, apolipoprotein A-I; PL, phospholipid; SUV, small unilamellar vesicle.

[a] Assuming a stock solution of 1.1 mg/ml apoA-I in PBS.

[b] Assuming a stock solution of 17.1 mg/ml PL in PBS. This yields a final concentration of 43 μg of PL per 100 μl of reaction, or ~ 5.6×10^{-4} M.

[c] The additional 15 μl was factored in to ensure enough sample for three separate 100 μl samples at each concentration of apoA-I after pipetting errors.

of vesicles that was included in each incubation (see below). Note that it is critical that the vesicle controls be diluted with the PBS/1% sodium cholate solution (not PBS alone), because the sodium cholate can significantly affect the quantum yield of the rhodamine probe (data not shown).

The CBQCA protein assay is then used to measure the amount of protein eluted from each column. This highly sensitive assay works by modifying free amines in the protein with a fluorescent adduct. Note that PBS was used for this assay because buffers that contain free amines, such as Tris-based buffers, will interfere with the protein assay. This assay was chosen because it can easily detect protein down to 10 μg/ml, and its fluorescence properties allow it to be measured in the presence of the rhodamine B probe on the PL without interference. A standard curve must be prepared, preferably on the same fluorescence microplate that contains the samples, that covers the concentration range of the protein used. We highly recommend that prequantified samples of the apolipoprotein under study be used for the standard curve, as we have found that the CBQCA assay can give disparate results between different proteins. The samples for the standard curve should be brought to the same volume (250 μl) as the other samples on the plate with the PBS/1% sodium cholate (which we have determined does not affect the assay significantly). Ten microliters of 40 mM KCN solution is then added to all samples, vesicle controls, and protein standards. After gentle vortexing of the plate, 10 μl of a 2 mM aqueous solution of CBQCA (in PBS) is added to each well and vortexed. The plate is covered and incubated in the dark for 1 h at room temperature and then subjected to two scans on a fluorescence plate reader. The first scan quantitates the eluted PL by exciting the rhodamine B fluorophor at 550 nm and monitoring emission at 590 nm. Our plate reader has an excitation filter at 544 nm and an emission filter at 590 nm, which worked well. The second scan quantitates the eluted protein by exciting the CBQCA product near 465 nm and monitoring at 550 nm. Our plate reader used a filter at 485 nm with emission at 538 nm. Control experiments showed no significant contribution of the PL signal to the protein signal and vice versa (data not shown).

Data analysis. The protein concentrations in each eluted sample ($[P_e]$) are then determined by simple linear regression analysis of the protein standards. The PL concentration in each eluted sample is determined by comparison with the vesicle control samples by the following formula:

$$[V_e] = I_e[V_t]/I_c \qquad (Eq.\ 1)$$

where $[V_e]$ represents the unknown concentration of vesicles (i.e., PL) present in the elution, I_e represents the fluorescence intensity of the eluted sample (in detector counts), $[V_t]$ represents the total concentration of vesicles initially added to the incubation and the vesicle control sample (in our case, 43 μg/100 μl), and I_c represents the fluorescence intensity of the control samples (detector counts). The accuracy of this determination was repeatedly verified by analysis of phosphorus in the samples (data not shown). Once $[P_e]$ and $[V_e]$ are known, the total amount of SUV-bound protein in the sample $[P_b]$ can be calculated by

$$[P_b] = [P_e]([V_t]/[V_e]) \qquad (Eq.\ 2)$$

See Appendix for a description of the equilibrium binding theory and the equations used to calculate the lipid binding parameters.

Other methods used to characterize the assay. Protein concentrations of apolipoprotein standards were determined by the Lowry procedure compared with standards of BSA (27). The PL content of the vesicles was determined by phosphorus analysis (28). Fluorescence energy transfer measurements were performed on a Photon Technology International Quantamaster spectrometer in photon-counting mode. Fluorescence analysis was carried out at 25°C in a semi-micro-quartz cuvette, and the emission and excitation band passes were 3.0 nm.

RESULTS

Assay development

Our goal was to produce a simple, robust assay capable of triplicate measurement of lipid binding parameters for multiple apolipoproteins. Once the overall strategy was conceptualized, two important issues had to be balanced. On the one hand, the chosen conditions had to allow for robust sample detection and reproducibility at each concentration. On the other hand, the overall consumption of apolipoprotein sample and reagents, such as the immobilized streptavidin resin, had to be minimized. Numerous pilot experiments were performed varying parameters such as the amount of streptavidin resin per well, the amount of SUV per reaction, the ratio of protein to SUV, the type and concentration of detergent required to completely elute the columns, etc. (data not shown). An example was the determination of the minimum amount of BT-PE required in the SUV to promote effective binding to the streptavidin beads. **Figure 2** shows that POPC vesicles minimally bound to the beads. However, as BT-PE was titrated into the SUV, the vesicles bound efficiently to the resin, reaching a maximum binding of 92–95%

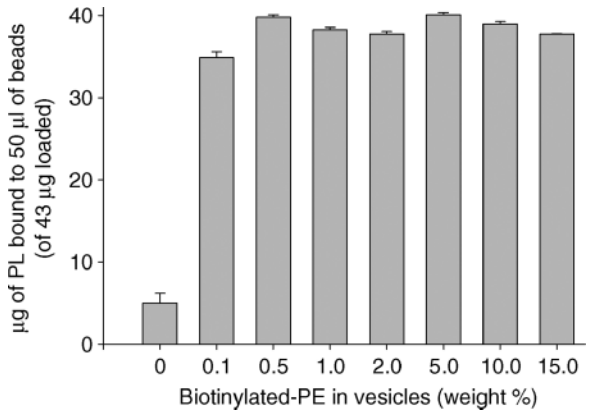

Fig. 2. Determination of the minimum amount of BT-PE required for effective binding of SUV to streptavidin beads. A total of 43 μg of POPC/BT-PE/Rhod-PE SUV was incubated with 50 μl of streptavidin bead slurry for 30 min at room temperature with intermittent vortexing. The mass percentage of BT-PE was varied as shown, with the mass of POPC reduced accordingly. Rhod-PE was always present at 0.5%. The columns were washed with 3 × 100 μl of PBS, and the Rhod-B fluorescence in the flow-through was compared with a sample of 43 μg of vesicles in a total of 350 μl of PBS that had not been passed down a column. The amount of lipid retained on the column was calculated and plotted versus the weight percentage of BT-PE in the vesicles. Each bar represents three samples, and the error bars represent ±1 sample SD.

with 0.5% BT-PE by weight. Experiments such as these resulted in the optimized protocol described in Experimental Procedures.

Assay characterization

Using the optimized protocol, a binding curve was generated for human plasma apoA-I (**Fig. 3**). The curve exhibited a rapid increase at low apoA-I concentrations, which saturates near 2 μM, corresponding to roughly six molecules of apoA-I per vesicle. As detailed in the Appendix, the data analysis assumes an equilibrium between lipid-free protein and protein bound to multiple identical sites on the vesicle, with no disruption of the vesicle morphology. To verify that the system was at equilibrium under the conditions of the assay, the kinetics of apoA-I binding to the vesicles was determined by fluorescent energy transfer experiments using vesicles that contained Dansyl-PE substituted for the Rhod-PE (**Fig. 4A**). Saturating concentrations of apoA-I, determined from Fig. 3, were used under the same conditions as for the assay. As the excited tryptophan residues of apoA-I associated with the SUV surface, energy transfer was measured by the fluorescence emission of the Dansyl probe. It is clear that apoA-I rapidly associated with the vesicles, reaching a maximal energy transfer in ~7 min after mixing. In contrast, BSA, which does not bind lipid surfaces, failed to induce energy transfer, despite containing a similar number of tryptophan residues. Figure 4B confirms that incubations for longer than the 30 min used in the protocol did not significantly increase the amount of protein associated with the vesicles. Figure 4C shows that saturating concentrations of apoA-I slightly decreased the retention time of the SUV on a gel filtration column, consistent with an increase in vesicle size attributable to the adsorbed apoA-I molecules. However, there was no evidence of vesicle rearrangement into small discoidal particles (which typically

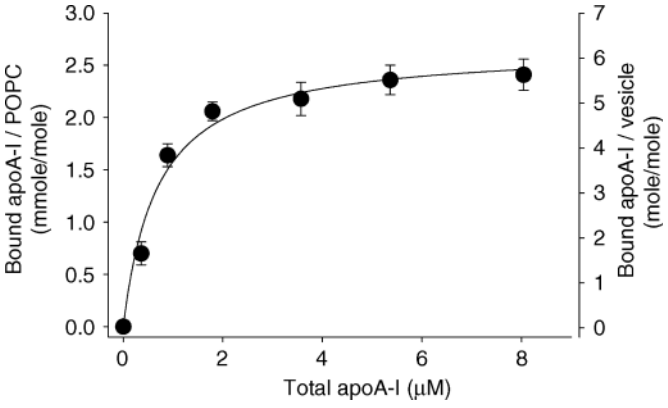

Fig. 3. Binding profile of human plasma apolipoprotein A-I (apoA-I) to SUVs. ApoA-I binding to 43 μg of SUV [99% POPC/0.5% BT-PE/0.5% Rhod PE (w/w)] in a volume of 100 μl of PBS (5.6×10^{-4} M PL) for 30 min at 25°C. The right axis shows the number of bound molecules of apoA-I per vesicle, assuming that each vesicle contains ~2,300 PL molecules (21). The solid line is a best fit to equation A6 (see Appendix). Each point represents the mean of three replicates, and the error bars represents ±1 SD.

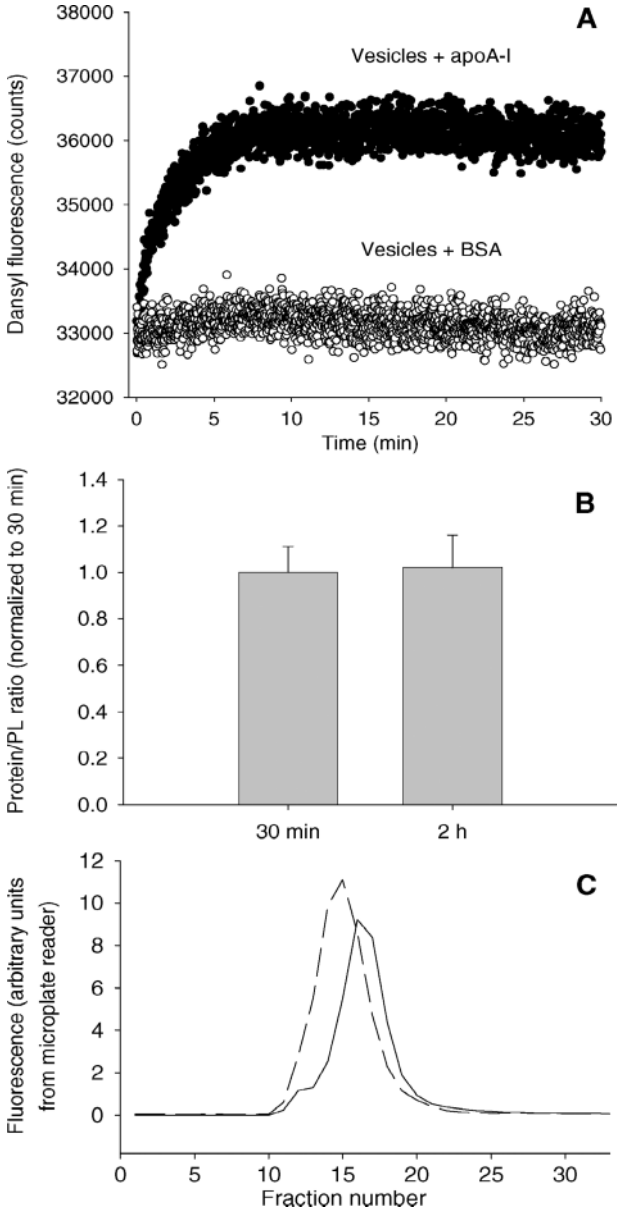

Fig. 4. Determination of the kinetics of apoA-I binding to SUV and the effect on vesicle morphology. A: SUVs were prepared and isolated as described for Fig. 2, except that the Rhod-PE was replaced with (5-dimethylamino-1-naphthanesulfonyl)-1,2 dioleoylphosphatidylethanolamine at the same mass percentage. A total of 301 μg of the vesicles was mixed with 158 μg of apoA-I in 700 μl of PBS. The sample was immediately placed in a spectrofluorometer and excited at 280 nm (to excite the tryptophan residues) while monitoring for fluorescence emission at 507 nm (the emission wavelength for the Dansyl label). The fluorescent energy transfer between the apoA-I tryptophan residues and the Dansyl probe as the protein was inserted into the vesicle bilayer is shown by the closed circles. The open circles show the same reaction containing BSA, which is not known to bind directly to PL vesicles. Each scan represents a single sample, but similar results were obtained in three separate runs. B: The bars show the total protein-to-PL ratio measured by the assay as described for Fig. 3, except that the incubation time for the protein with the vesicles was either 30 min or 2 h. The data are normalized to the 30 min results. Each result represents a mean of three observations ±1 SD. C: A total of 22.5 μg of apoA-I was incubated with 43 μg of SUV (99% POPC, 0.5% BT-PE, 0.5% Rhod-PE) for 30 min at 25°C and then applied to a Superose 6 gel filtration column. The resulting fractions were monitored for the presence of Rhod-PE on a fluorescence microplate reader and plotted (dotted line). The solid line shows the vesicle profile with no addition of apoA-I.

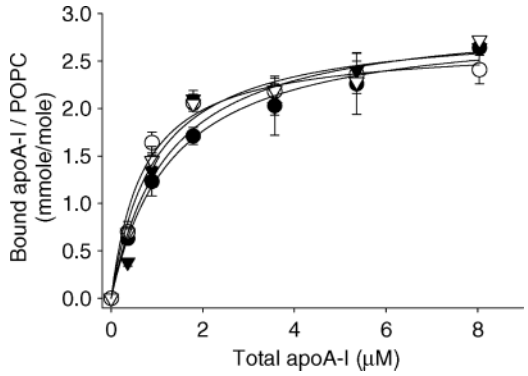

Fig. 5. Determination of assay reproducibility using apoA-I. The figure is organized similarly to Fig. 3. Profiles a (closed circles), b (open circles), and c (closed triangles) were each generated on a different day (over a 6 week period) with the same protocol using the same preparation of apoA-I. Profile d (open triangles) was generated in the same experiment as profile b but used an independent preparation of apoA-I. Each point represents the mean of three replicates, and the error bars represent ±1 SD. The lipid binding parameters of each trace are listed in Table 2.

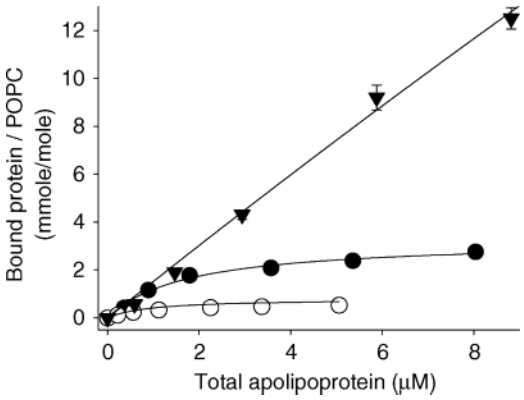

Fig. 6. Use of the assay to measure the lipid binding characteristics of other apolipoproteins. The figure is organized similarly to Fig. 3. Closed circles, human plasma apoA-I; open circles, recombinant human apoA-IV; closed triangles, human plasma apoA-II. Each point represents the mean of three replicates, and the error bars represent ±1 SD.

appear around fraction 25). These data indicate that the binding of apoA-I to the SUV easily reached equilibrium by 30 min without significant modification of the vesicles.

To get a sense of assay reproducibility, a series of binding curves were generated on different days (over a 6 week period) using the same preparation of human plasma apoA-I and the same protocol. The results are shown in **Fig. 5**, and the resulting binding parameters are listed in **Table 2**. A binding curve for an independent preparation of human apoA-I is also shown. In general, the curves were superimposable within the error bars of each measurement. Table 2 shows that all three experiments with the same apoA-I preparation resulted in an average K_d of 1.1 μM and an n of 2.9 mmol apoA-I/mol PL. Assuming 2,300 (21) molecules of PL per vesicle, this indicates that there are six to seven binding sites for apoA-I per vesicle. The standard deviations for both the K_d and n indicated a reasonable interassay reproducibility. The calculated parameters for the independent preparation of apoA-I also fell within these ranges. Table 2 also shows that the calculated K_d values agreed quite well with those reported by Yokoyama et al. (21) for apoA-I association with egg yolk phosphatidylcholine vesicles (1.1 vs. 0.9 μM). However, the number of molecules per vesicle at saturation was somewhat higher in our assay (seven vs. four).

Application of the assay

Having established that the assay can effectively and reproducibly derive equilibrium binding parameters for human plasma apoA-I, we measured binding parameters for other apolipoproteins. We chose human plasma apoA-II because it is known to exhibit a higher lipid binding affinity than apoA-I (29, 30). By contrast, apoA-IV is known to be a significantly poorer lipid binder than apoA-I (7, 14, 31). **Figure 6** and **Table 3** show that apoA-I exhibited saturated binding, with parameters that were in agreement with those in Table 2. Interestingly, bacterially expressed human apoA-IV bound to the vesicles with a K_d that, on a molar basis, was similar to that of apoA-I. However, the saturation point was much lower, with only one to two molecules binding per vesicle. In contrast, human plasma apoA-II appeared to avidly bind to the vesicles and failed to saturate at the concentrations used in the assay. **Figure 7** shows that apoA-IV behaved like apoA-I in that it had fully

TABLE 2. Binding parameters for human plasma apoA-I to SUV shown in Fig. 5

		K_d		n	
Sample[a]	Symbol[b]	μM	g/l	mmol apolipoprotein/mol PL	molecules/vesicle[c]
ApoA-I (a)	Closed circles	1.33 ± 0.19	0.037 ± 0.005	2.93 ± 0.21	6.74 ± 0.47
ApoA-I (b)	Open circles	0.70 ± 0.06	0.021 ± 0.002	2.68 ± 0.14	6.16 ± 0.31
ApoA-I (c)	Closed triangles	1.24 ± 0.23	0.035 ± 0.007	3.00 ± 0.07	6.91 ± 0.17
Average		1.09 ± 0.34	0.031 ± 0.009	2.87 ± 0.17	6.66 ± 0.40
ApoA-I (d)	Open triangles	0.93 ± 0.11	0.026 ± 0.003	2.88 ± 0.11	6.62 ± 0.25
Yokoyama et al. (21)		0.90	0.025	1.74	4.0

K_d, equilibrium dissociation constant; n, maximal binding of an apolipoprotein to a given lipid surface.
[a] Samples a, b, and c were run with the same preparation of purified human plasma apoA-I under identical conditions on different days. Sample d represents an independent preparation of apoA-I assayed on the same day as sample b.
[b] Refers to the traces in Fig. 5.
[c] Assuming 2,300 molecules of PL per SUV (21).

TABLE 3. Binding parameters for human plasma apoA-I to SUV shown in Figs. 6 and 8

Sample[a]	Symbol[b]	K_d		n	
		μM	g/l	mmol apolipoprotein/mol PL	molecules/vesicle[c]
Fig. 6					
ApoA-I	Closed circles	1.30 ± 0.19	0.036 ± 0.005	2.83 ± 0.06	6.52 ± 0.13
ApoA-IV	Open circles	1.57 ± 0.55	0.070 ± 0.025	0.63 ± 0.09	1.44 ± 0.20
ApoA-II	Closed triangles	N.D.[d]	N.D.	N.D.	N.D.
Fig. 8					
ApoA-I	Closed circles	0.93 ± 0.11	0.026 ± 0.003	2.88 ± 0.11	6.62 ± 0.25
ApoA-I Δ221–243	Closed squares	4.60 ± 0.61	0.116 ± 0.150	1.96 ± 0.18	4.51 ± 0.41
ApoA-IV	Open squares	1.25 ± 0.15	0.056 ± 0.007	0.85 ± 0.08	1.95 ± 0.19
ApoA-IV F334A	Open circles	0.041 ± 0.003	$1.6 \times 10^{-3} \pm 0.5 \times 10^{-3}$	1.58 ± 0.03	3.63 ± 0.06

[a] Wild-type apoA-I and apoA-II were purified from human plasma. ApoA-IV and all mutants were human proteins expressed in bacteria.
[b] Refers to the traces in Figs. 6 and 8.
[c] Assuming 2,300 molecules of PL per SUV (21).
[d] Not determined. Coefficients were not calculated because the binding failed to reach equilibrium and because apoA-II clearly disrupted the SUV (Fig. 7D).

bound to the vesicles within 30 min and did not significantly change the vesicle size. By contrast, 30 min was not sufficient for the maximal association of apoA-II with the vesicles (Fig. 7C), and it was clear from the gel filtration analysis that this apolipoprotein disrupted the vesicles, repackaging them into smaller discoidal particles within the 30 min incubation (Fig. 7D). Further experiments showed that apoA-II almost completely converted the vesicles to discs by 24 h (data not shown). This indicates that apoA-II binding cannot be accurately measured under the assumptions used in this assay (see Discussion).

To further probe the utility of the assay, we measured the binding parameters of apoA-I and apoA-IV mutants that have previously been shown to exhibit altered lipid binding. Deletion of the C-terminal amphipathic helix of apoA-I is known to dramatically reduce both its lipid affinity and its cholesterol efflux capacity (6, 32–34). Consistent with this, **Fig. 8A** and Table 3 show that the bacterially expressed deletion mutant of apoA-I (Δ221–243) was significantly less effective at binding lipid than the intact plasma form. This is reflected both in a 32% reduction in n and a 4- to 5-fold increase in K_d. This indicates that the

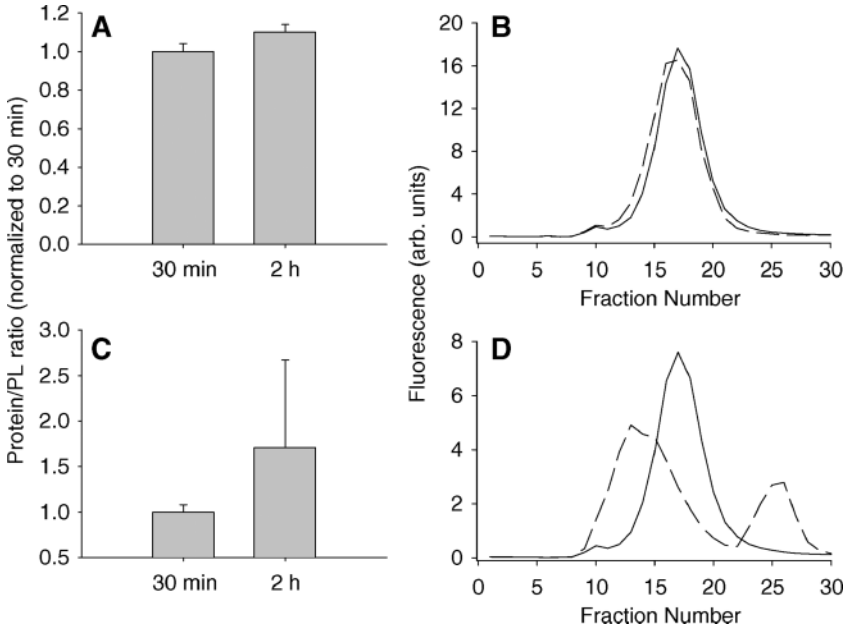

Fig. 7. Characterization of the binding of apoA-IV and apoA-II to the vesicles used in the biotin-capture lipid affinity (BCLA) assay. A: Effect of incubation time on the binding of 22.5 μg of recombinant human apoA-IV to 43 μg vesicles under the same conditions described for Fig. 4B. The data are normalized to the 30 min results. Each result represents a mean of three observations ±1 SD. B: A total of 22.5 μg of apoA-IV was incubated with 43 μg of SUV for 30 min and analyzed on a Superose 6 gel filtration column as described for Fig. 4C (dotted line). The solid line shows the vesicles without the addition of apoA-IV. C: The same experiment shown in A, except that 22.5 μg of human plasma apoA-II was incubated with 43 μg of vesicles. D: Superose 6 gel filtration profile for apoA-II incubated with vesicles (dotted line) and the vesicles alone (solid line). The lipid binding parameters are listed in Table 3.

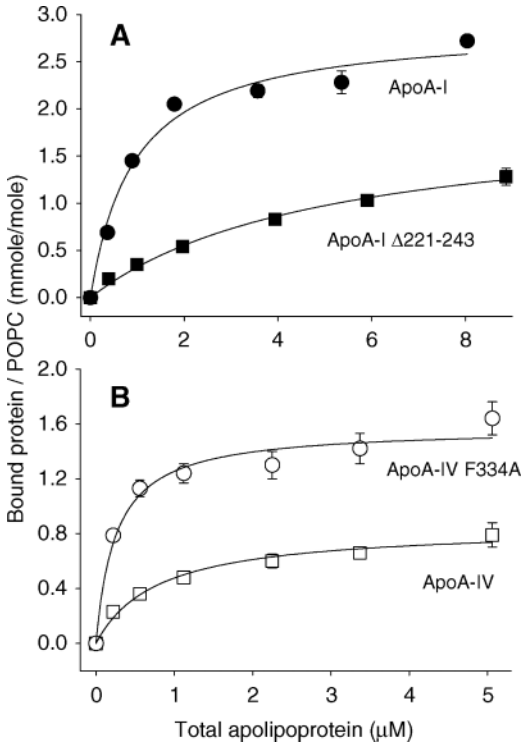

Fig. 8. Use of the BCLA assay to study the lipid binding parameters of apoA-I and apoA-IV mutant proteins. The figure is organized similarly to Fig. 3. Each point represents the mean of three replicates ±1 SD. A: Human plasma apoA-I compared with a bacterially expressed mutant that lacks the C-terminal lipid binding helix (6). B: Bacterially expressed wild-type human apoA-IV (7) compared with a point mutant that is known to bind dimyristoylphosphatidylcholine liposomes with higher avidity than the wild-type protein (35). The lipid binding parameters are listed in Table 3.

deletion of the C-terminal amphipathic helix in apoA-I reduced the vesicle capacity for the protein and also significantly reduced the affinity of the protein for the available binding sites. In the case of apoA-IV, we recently identified a single point mutation (F334A) that promotes a striking increase in apoA-IV lipid binding affinity, most likely through a conformational mechanism (35). Figure 8B shows that the vesicles exhibited a significantly greater capacity for this mutant compared with wild-type apoA-IV. Comparison of the parameters in Table 3 confirms a 2-fold increase in n along with a 30-fold decrease in K_d. Control experiments showed that none of these variants disrupted vesicle morphology and were maximally bound to the vesicles by 30 min (data not shown).

DISCUSSION

This report presents a straightforward lipid binding assay that is capable of rapidly and reproducibly determining the equilibrium binding parameters of lipid-associating proteins. The separation of bound versus free protein is performed in parallel and within seconds, offering advantages over previous gel filtration methods that separate more slowly (on the order of several minutes) and are performed sequentially. Using the BCLA assay, we have measured triplicate binding parameters for eight separate apolipoproteins across seven different concentrations in 3.5 h. Importantly, the sensitivity of the fluorescence lipid and protein detection allows the consumption of only 120 μg of apolipoprotein for each protein being measured, reducing the amount of recombinant protein that needs to be purified for characterization. Furthermore, the assay uses relatively basic equipment and is thus available to laboratories that might not have ready access to sophisticated instrumentation, such as calorimeters, surface balances, spectrofluorimeters, or capillary electrophoresis devices.

The assay can be used with any apolipoprotein without the need for labeling, modification, antibody-based detection, or the presence of any particular amino acid such as tryptophan. However, as discussed in the Appendix, the equilibrium analysis depends on the assumption that the apolipoprotein binds to the membrane in a single event and without disrupting the vesicles. We found that apoA-II clearly promoted additional lipid reorganization events after it associated with the vesicle, precluding a rigorous determination of binding parameters for this protein. This observation highlights the importance of performing characterization experiments like those shown in Fig. 4, especially on proteins or mutants that display remarkably robust lipid binding capacity, before the determined parameters are given detailed consideration.

The BCLA has several advantages over the commonly used DMPC turbidometric assay. First, it provides broadly applicable equilibrium binding constants for a well-defined molecular event (i.e., the binding of the apolipoprotein to the surface of a uniform population of vesicles). The DMPC assay, in contrast, is a kinetic assay that measures the end point of a multistep event involving the binding of the apolipoprotein to the liposome surface, disruption of the bilayer, and reorganization into small discoidal particles (23). Thus, the DMPC assay does not directly address lipid binding affinity per se but is more of a qualitative index of the ability of a given protein to solubilize a planar lipid surface. Another advantage of the BCLA assay over the DMPC assay is reproducibility. The disruption of DMPC liposomes depends on the formation of surface packing defects formed in the lipid at the gel-liquid crystal transition temperature (24.5°C). Even slight deviations from this temperature can have dramatic effects on the kinetics of the solubilization. This, combined with heterogeneity between liposome preparations, makes results from different experimental runs (even on the same day) nearly impossible to compare. The best way around this problem has been to compare apolipoproteins within the same run. In contrast, the BCLA assay offers better interassay reproducibility, allowing historical comparisons without the need to run all proteins at the same time.

Table 2 shows that the K_d determined for apoA-I matched quite closely with those from a study performed by Yokoyama et al. (21). However, the number of binding sites per vesicle was noticeably higher in our measure-

ments (seven molecules of apoA-I per vesicle, vs. four in the previous study). Several groups have measured this parameter in comparable vesicle systems (composed of either POPC or egg yolk phosphatidylcholine), with the values ranging from three to five (12, 21, 26). We have determined that the higher value of n is not an artifact of the streptavidin column separation strategy, because an analysis of an incubation containing an excess of apolipoprotein on a gel filtration column (Fig. 4C) resulted in the same number of apoA-I molecules per vesicle that we measured in the BCLA assay (data not shown). Thus, we suggest that our values of n may be somewhat higher because of the presence of the two probe lipids in the SUV. Although constituting only 1% of the vesicle mass, it is possible that the different head groups (phosphatidylethanolamine vs. phosphatidylcholine), acyl chain composition, or the presence of the probe itself may slightly affect the vesicle's capacity for the apolipoprotein. Indeed, when cholesterol is titrated into egg yolk phosphatidylcholine vesicles, the number of apoA-I molecules bound per vesicle can increase by 2-fold (21). Increasing the amount of the labeled PLs in our system did not result in further increases in the n parameter (data not shown), although there may be a threshold beyond which further increases have no effect. In any case, the use of a standardized vesicle preparation ensures the comparability of experiments performed with our protocol.

We should note that one drawback of this assay is that the streptavidin resin is somewhat expensive. Because the streptavidin/biotin interaction is so strong (36), we have not found a practical way to release the bound BT-PE from the columns to reuse it for new analyses. A typical 5 ml bottle of resin can provide up to 100 assays or about five concentration curves in triplicate. At current prices, this is on the order of $60–70 per apolipoprotein analyzed. Current work in our laboratory is studying the feasibility of using nitrated forms of avidin that are capable of releasing bound biotin at high pH. Nevertheless, we would argue that the time saved using the BCLA assay versus other more labor-intensive methods may compensate for the materials cost.

Finally, it is worth mentioning that this assay may prove useful for high-throughput screens designed to detect lipid binding variants in random mutagenesis studies of recombinant apolipoproteins. Rather than deriving binding constants from entire concentration curves, one or two points near the known K_d of the wild-type protein can be selected to compare hundreds of mutants generated by high-throughput protein expression techniques.

APPENDIX

The lipid binding data in this study were analyzed with the following assumptions: *a*) the SUVs were treated as a multivalent uniform receptor with a finite number of identical and noninteracting binding sites; *b*) the apolipoprotein binds to the vesicles reaching a single equilibrium; and *c*) the apolipoprotein does not disrupt the vesicle structure upon binding. According to classical univalent equilibrium binding theory, the apolipoprotein (P) interacts with the vesicle (V) in a reversible manner:

$$V + P \leftrightarrow VP \qquad (Eq.\ A1)$$

Equilibrium constants for the binding (K_b) and the dissociation (K_d) events are then defined by

$$K_b = [VP]/([V][P]) \text{ and } K_d = ([V][P])/[VP] \qquad (Eq.\ A2)$$

The K_d can be expressed in terms of [VP] by

$$[VP] = ([V][P])/K_d \qquad (Eq.\ A3)$$

Using basic mass balance principles, the ratio of bound apolipoprotein (P_b) to the total amount of vesicles in the reaction (V) can be expressed as

$$[P_b]/[V] = [VP]/([V] + [VP]) \qquad (Eq.\ A4)$$

Substituting equation A3 into equation A4 results in

$$[Pb]/[V] = [P]/(K_d + [P]) \qquad (Eq.\ A5)$$

For n identical binding sites in a multisite receptor such as the vesicles, $[P_b]/[V]$ equals n times the binding of the apolipoprotein by a single isolated site. Thus,

$$[P_b]/[V] = n([P]/(K_d + [P])) \qquad (Eq.\ A6)$$

where $[P_b]$ is the concentration of vesicle-bound apolipoprotein, [V] is the total lipid concentration of the vesicles in the reaction, and [P] is the total concentration of apolipoprotein added to the reaction. K_d is a general equilibrium dissociation constant, and n represents the maximum amount of $[P_b]/[V]$. A straightforward way to visualize the data is by plotting $[P_b]/[V]$ as a function of [P] (Fig. 3). The binding isotherms for all figures in this article were generated by a nonlinear fit of the data to equation A6 using Sigma Plot (Jandel Scientific).

This work was supported by Grants HL-67093 and HL-62542 (W.S.D.) from the National Institutes of Health and a predoctoral fellowship from the Ohio Valley Affiliate of the American Heart Association (K.P.). The authors thank Dr. Henry Pownall from the Baylor College of Medicine for helpful comments and discussion.

REFERENCES

1. Lee, J. Y., and J. S. Parks. 2005. ATP-binding cassette transporter AI and its role in HDL formation. *Curr. Opin. Lipidol.* **16:** 19–25.
2. Jian, B., M. de la Llera-Moya, Y. Ji, N. Wang, M. C. Phillips, J. B. Swaney, A. R. Tall, and G. H. Rothblat. 1998. Scavenger receptor class B type I as a mediator of cellular cholesterol efflux to lipoproteins and phospholipid acceptors. *J. Biol. Chem.* **273:** 5599–5606.
3. Wang, N., D. Lan, W. Chen, F. Matsuura, and A. R. Tall. 2004. ATP-

binding cassette transporters G1 and G4 mediate cellular cholesterol efflux to high-density lipoproteins. *Proc. Natl. Acad. Sci. USA.* **101:** 9774–9779.
4. Oram, J. F., R. M. Lawn, M. R. Garvin, and D. P. Wade. 2000. ABCA1 is the cAMP-inducible apolipoprotein receptor that mediates cholesterol secretion from macrophages. *J. Biol. Chem.* **275:** 34508–34511.
5. Green, P. H., R. M. Glickman, J. W. Riley, and E. Quinet. 1980. Human apolipoprotein A-IV. Intestinal origin and distribution in plasma. *J. Clin. Invest.* **65:** 911–919.
6. Panagotopulos, S. E., S. R. Witting, E. M. Horace, D. Y. Hui, J. N. Maiorano, and W. S. Davidson. 2002. The role of apolipoprotein A-I helix 10 in apolipoprotein-mediated cholesterol efflux via the ATP-binding cassette transporter ABCA1. *J. Biol. Chem.* **277:** 39477–39484.
7. Pearson, K., H. Saito, S. C. Woods, S. Lund-Katz, P. Tso, M. C. Phillips, and W. S. Davidson. 2004. Structure of human apolipoprotein A-IV: a distinct domain architecture among exchangeable apolipoproteins with potential functional implications. *Biochemistry.* **43:** 10719–10729.
8. Gazzara, J. A., M. C. Phillips, S. Lund-Katz, M. N. Palgunachari, J. P. Segrest, G. M. Anantharamaiah, and J. W. Snow. 1997. Interaction of class A amphipathic helical peptides with phospholipid unilamellar vesicles. *J. Lipid Res.* **38:** 2134–2146.
9. Pownall, H. J., F. J. Hsu, M. Rosseneu, H. Peeters, A. M. Gotto, and R. L. Jackson. 1977. Thermodynamics of lipid protein associations. Thermodynamics of helix formation in the association of high density apolipoprotein A-I (apoA-I) to dimyristoyl phosphatidylcholine. *Biochim. Biophys. Acta.* **488:** 190–197.
10. Derksen, A., D. Gantz, and D. M. Small. 1996. Calorimetry of apolipoprotein-A1 binding to phosphatidylcholine-triolein-cholesterol emulsions. *Biophys. J.* **70:** 330–338.
11. Rosseneu, M., F. Soetewey, G. Middelhoff, H. Peeters, and W. V. Brown. 1976. Studies of the lipid binding characteristics of the apolipoproteins from human high density lipoprotein. II. Calorimetry of the binding of apo AI and apo AII with phospholipids. *Biochim. Biophys. Acta.* **441:** 68–80.
12. Arnulphi, C., L. Jin, M. A. Tricerri, and A. Jonas. 2004. Enthalpy-driven apolipoprotein A-I and lipid bilayer interaction indicating protein penetration upon lipid binding. *Biochemistry.* **43:** 12258–12264.
13. Ibdah, J. A., K. E. Krebs, and M. C. Phillips. 1989. The surface properties of apolipoproteins A-I and A-II at the lipid/water interface. *Biochim. Biophys. Acta.* **1004:** 300–308.
14. Weinberg, R. B., J. A. Ibdah, and M. C. Phillips. 1992. Adsorption of apolipoprotein A-IV to phospholipid monolayers spread at the air/water interface. A model for its labile binding to high density lipoproteins. *J. Biol. Chem.* **267:** 8977–8983.
15. Weinberg, R. B., V. R. Cook, J. A. DeLozier, and G. S. Shelness. 2000. Dynamic interfacial properties of human apolipoproteins A-IV and B-17 at the air/water and oil/water interface. *J. Lipid Res.* **41:** 1419–1427.
16. Breyer, E. D., S. Howard, N. Raje, S. Allison, R. Apkarian, W. V. Brown, and J. K. Strasters. 2003. Study of lipid and apolipoprotein binding interactions using vesicle affinity capillary electrophoresis. *Anal. Chem.* **75:** 5160–5169.
17. Drin, G., M. Mazel, P. Clair, D. Mathieu, M. Kaczorek, and J. Temsamani. 2001. Physico-chemical requirements for cellular uptake of pAntp peptide. Role of lipid-binding affinity. *Eur. J. Biochem.* **268:** 1304–1314.
18. Silvius, J. R. 1999. Fluorescence measurement of lipid-binding affinity and interbilayer transfer of bimane-labeled lipidated peptides. *Methods Mol. Biol.* **116:** 177–186.
19. Isenberg, G., S. Doerhoefer, D. Hoekstra, and W. H. Goldmann. 2002. Membrane fusion induced by the major lipid-binding domain of the cytoskeletal protein talin. *Biochem. Biophys. Res. Commun.* **295:** 636–643.
20. Kolusheva, S., T. Shahal, and R. Jelinek. 2000. Peptide-membrane interactions studied by a new phospholipid/polydiacetylene colorimetric vesicle assay. *Biochemistry.* **39:** 15851–15859.
21. Yokoyama, S., D. Fukushima, J. P. Kupferberg, F. J. Kezdy, and E. T. Kaiser. 1980. The mechanism of activation of lecithin:cholesterol acyltransferase by apolipoprotein A-I and an amphiphilic peptide. *J. Biol. Chem.* **255:** 7333–7339.
22. Surewicz, W. K., R. M. Epand, H. J. Pownall, and S. W. Hui. 1986. Human apolipoprotein A-I forms thermally stable complexes with anionic but not with zwitterionic phospholipids. *J. Biol. Chem.* **261:** 16191–16197.
23. Segall, M. L., P. Dhanasekaran, F. Baldwin, G. M. Anantharamaiah, K. H. Weisgraber, M. C. Phillips, and S. Lund-Katz. 2002. Influence of apoE domain structure and polymorphism on the kinetics of phospholipid vesicle solubilization. *J. Lipid Res.* **43:** 1688–1700.
24. Lund-Katz, S., and M. C. Phillips. 1986. Packing of cholesterol molecules in human low-density lipoprotein. *Biochemistry.* **25:** 1562–1568.
25. Davidson, W. S., and G. M. Hilliard. 2003. The spatial organization of apolipoprotein A-I on the edge of discoidal high density lipoprotein particles: a mass spectrometry study. *J. Biol. Chem.* **278:** 27199–27207.
26. Davidson, W. S., W. V. Rodrigueza, S. Lund-Katz, W. J. Johnson, G. H. Rothblat, and M. C. Phillips. 1995. Effects of acceptor particle size on the efflux of cellular free cholesterol. *J. Biol. Chem.* **270:** 17106–17113.
27. Lowry, O. H., N. J. Rosenbrough, A. L. Farr, and R. J. Randall. 1951. Protein measurement with the Folin phenol reagent. *J. Biol. Chem.* **193:** 265–275.
28. Sokoloff, L., and G. H. Rothblat. 1974. Sterol to phospholipid molar ratios of L cells with qualitative and quantitative variations of cellular sterol. *Proc. Soc. Exp. Biol. Med.* **146:** 1166–1172.
29. Labeur, C., G. Lambert, T. Van Cauteren, N. Duverger, B. Vanloo, J. Chambaz, J. Vandekerckhove, G. Castro, and M. Rosseneu. 1998. Displacement of apo A-I from HDL by apo A-II or its C-terminal helix promotes the formation of pre-beta1 migrating particles and decreases LCAT activation. *Atherosclerosis.* **139:** 351–362.
30. Edelstein, C., M. Halari, and A. M. Scanu. 1982. On the mechanism of the displacement of apolipoprotein A-I by apolipoprotein A-II from the high density lipoprotein surface. Effect of concentration and molecular forms of apolipoprotein A-II. *J. Biol. Chem.* **257:** 7189–7195.
31. Weinberg, R. B., and M. S. Spector. 1985. Structural properties and lipid binding of human apolipoprotein A-IV. *J. Biol. Chem.* **260:** 4914–4921.
32. Minnich, A., X. Collet, A. Roghani, C. Cladaras, R. L. Hamilton, C. J. Fielding, and V. I. Zannis. 1992. Site-directed mutagenesis and structure-function analysis of the human apolipoprotein A-I. Relation between lecithin-cholesterol acyltransferase activation and lipid binding. *J. Biol. Chem.* **267:** 16553–16560.
33. Ji, Y., and A. Jonas. 1995. Properties of an N-terminal proteolytic fragment of apolipoprotein AI in solution and in reconstituted high density lipoproteins. *J. Biol. Chem.* **270:** 11290–11297.
34. Gillotte, K. L., M. Zaiou, S. Lund-Katz, G. M. Anantharamaiah, P. Holvoet, A. Dhoest, M. N. Palgunachari, J. P. Segrest, K. H. Weisgraber, G. H. Rothblat, et al. 1999. Apolipoprotein-mediated plasma membrane microsolubilization. Role of lipid affinity and membrane penetration in the efflux of cellular cholesterol and phospholipid. *J. Biol. Chem.* **274:** 2021–2028.
35. Pearson, K., M. R. Tubb, M. Tanaka, X. Q. Zhang, P. Tso, R. B. Weinberg, and W. S. Davidson. 2005. Specific sequences in the N- and C-termini of apolipoprotein A-IV modulate its conformation and lipid association. *J. Biol. Chem.* **280:** 38576–38582.
36. Eakin, R. E., E. E. Snell, and R. J. Williams. 1941. The concentration and activity of avidin, the injury-producing protein in raw egg white. *J. Biol. Chem.* **140:** 535–543.